

Structure and magnetic properties of FePt/B₄C multilayer thin films: Role of the compositional elements intermixing

M. J. Zhou and Quan Li^{a)}

Department of Physics, The Chinese University of Hong Kong, Shatin, New Territory, Hong Kong

F. J. Yang, H. B. Wang, and H. Wang^{b)}

Faculty of Physics and Electronic Technology, Hubei University, Wuhan 430062,

People's Republic of China and Key Laboratory of Ferro- and Piezo-electric Materials and Devices, Hubei University, Wuhan 430062, People's Republic of China

D. Tang

FEI Company, Eindhoven NL-5651, The Neitherlands

(Received 2 April 2007; accepted 20 June 2007; published online 9 August 2007)

FePt/B₄C multilayer thin films were deposited using magnetron sputtering with different boron carbide layer thicknesses. Experimental results suggest that the B₄C layers effectively serve as spacers to separate the FePt layers, making the multilayer configuration stable even after film annealing at elevated temperatures. On the other hand, B and C are found to incorporate into the FePt layer, which is responsible for the FePt grain growth confinement and grain separation, and eventually affects the magnetic properties of the composite film. © 2007 American Institute of Physics. [DOI: 10.1063/1.2757597]

In ultrahigh-density magnetic recording, media with small grains size and weak intergrain exchange coupling are desired to achieve the high storage density and adequate signal-to-noise ratio simultaneously. Among numerous choices of the recording media, equiatomic FePt nanoparticle with the L1₀ ordered structure has received intense research attention due to its high magnetoanisotropy energy (K_u), serving as one of the possible solutions to overcome superparamagnetism associated with finite grain size.¹⁻⁹

FePt nanocrystals synthesized at room temperature usually have a magnetically soft face centered-cubic (fcc) phase, which can transform to the L1₀ ordered face-centered-tetragonal (fct) phase after thermal annealing at elevated temperatures.^{10,11} Nevertheless, the high processing temperature promotes grain growth, which results in larger particle size and wider size distributions. Alloying with a certain third elements¹² or growing on a specific substrate layer¹³ is found to be effective in reducing the fcc-fct transition temperature. Another way to constrain the growth of FePt particles is utilizing a composite film configuration (such as dispersing FePt particles in a matrix film).^{8-10,14,15} Among these methods, the nanocomposite films are of particular interest. Not only it has been demonstrated that fine FePt grains (<10 nm) with coercivity of ~4 kOe form in the composite films but also that the intergrain interactions are reduced. This could lead to lower media noise due to the isolation of the magnetic particles by the nonmagnetic matrix. Nevertheless, the role of compositional elements intermixing on the properties of the film remains unclear.

In the present study, FePt/B₄C multilayer composite films were fabricated as a feasible system in investigating the element intermixing effect on the film coercivity and exchange coupling. An optimum film configuration is identified, in which a coercivity value at 7500 Oe and low exchange coupling among the individual magnetic layers as

well as the magnetic grains in each layer are achieved with FePt grain size at ~9 nm.

The FePt/B₄C composite films were deposited by magnetron sputtering at ambient temperature onto Si (001) substrates. Three 2.5 in. targets (B₄C 99.5%, Fe, 99.9%, Pt 99.9%, Kurt J. Company) were used as the source material, and the multilayer thin films were deposited by rotating the substrate to the three targets successively. The base pressure of the chamber was 2.0×10^{-4} Pa and a total pressure is maintained at 0.5 Pa during sputtering. Pure FePt thin film samples were firstly deposited to find out the optimum deposition condition to achieve the 1/1 Fe/Pt ratio. In a standard procedure, the as-deposited samples started with a 10 nm B₄C buffer layer on the substrate to avoid reaction between the metallic elements with the Si substrate. After that, 5 nm Fe/5 nm Pt/ x nm B₄C multilayer composite films were grown for six periods, with x ranging from 1 to 5 nm in the sample series. After deposition, all of the as-deposited films were annealed at 500 °C for 30 min in vacuum ($\sim 10^{-4}$ Pa).

The chemical composition of samples was examined by x-ray photoelectron spectroscopy [(XPS), PHI, Quantum 2000]. The crystallinity and the microstructure of the films were characterized by x-ray diffraction [(XRD), Bruker D5] and transmission electron microscopy [(TEM), Tecnai G2 FEG]. Both energy dispersive x-ray (EDX) spectrometer and electron energy loss spectrometer (EELS) (GIF) attached to the same microscope were used to obtain the compositional scanning profiles of the multilayer films. An ~3 Å electron probe is used during the EDX/EELS line scan, and the scanning step is maintained at 5 Å. The magnetic properties were measured with a vibrating sample magnetometer (Oxford instruments).

XPS measurements on an annealed pure FePt films reveal a close to 1/1 ratio of the Fe/Pt (Fe _{x} Pt_{100- x} , with $x=50 \pm 3$), which appears to be the best composition to yield the highest coercivity.¹⁶ The XRD results of all the multilayer films are similar in terms of the peak positions, but with different full widths at half maximum. A representative XRD pattern (multilayer film with 2 nm B₄C layer) is

^{a)} Author to whom correspondence should be addressed; electronic mail: liquan@phy.cuhk.edu.hk

^{b)} Electronic mail: liquan@126.com

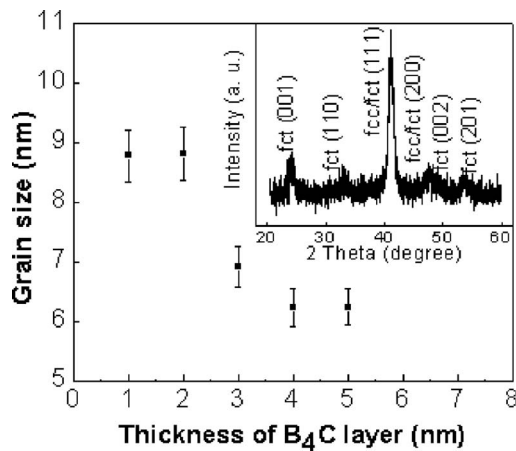


FIG. 1. Plot of the grain size change as a function of the B_4C layer as deduced by XRD analysis and a typical XRD pattern (taken from multilayer film with 2 nm B_4C layer) can be found in the inset of the figure.

shown in the inset of Fig. 1, confirming the existence of the fct phase in the multilayer film. The grain sizes of the FePt in the composite films are estimated using the most intense diffraction peak in the XRD spectra based on the Scherrer formula. Figure 1 plots the FePt grain size in the multilayer composite film change with the B_4C layer thickness. The grain sizes of FePt are found to be similar (~ 8.8 nm) for B_4C layer thickness less than 2 nm in the composite film. Increase in the B_4C layer thickness to 3 nm leads to a grain size decrease to ~ 7.0 nm. Further increase in the B_4C layer thickness to 4 nm and above has little effect on the grain size of FePt, which remains at ~ 6.5 nm.

The multilayer structure in the composite film is clearly disclosed by the TEM study. One can find that the multilayers are barely discernable in film deposited with 1 nm B_4C layer [Fig. 2(a)]. With the B_4C layer thickness increase, a distinct multilayer configuration can be observed [Fig. 2(b)]. This is further confirmed by the dark field image taken with a high angle annular dark field detector [Figs. 2(c) and 2(d)]. The light/dark contrasts in the images suggest the Fe–Pt rich and the B–C rich layers, respectively. Nevertheless, the interface in between the individual B_4C and the FePt layer is never smooth, and an interfacial roughness of ~ 1 nm can be estimated from the high-resolution TEM images [Figs. 2(e) and 2(f)]. The high-resolution images also disclose the amorphous nature of the B_4C layer, which explains the absence of crystalline reflections from such a phase in the XRD results.

The distributions of the compositional elements along the films' normal are examined by EDX (for Fe and Pt) and EELS (for B and C) line scan using scanning TEM [Figs. 2(g) and 2(h)]. The abundance modulation of B and C becomes obvious only at larger B_4C layer thickness (≥ 2 nm) when signals from B and C also become detectable in the FePt layer. The modulation of Fe in a layered pattern is absent at small B_4C layer thickness ($=1$ nm) and become discernable when B_4C grows thick. As a comparison, distinct abundance modulation of Pt is always observed in all the composite films. Unlike B and C, the Fe and Pt signals are mainly restricted in the FePt layers for samples with B_4C layer thickness greater than 2 nm.

The chemical and structural characterizations of the composite films suggest the intermixing of compositional elements in the multilayer films. Such intermixing is expected

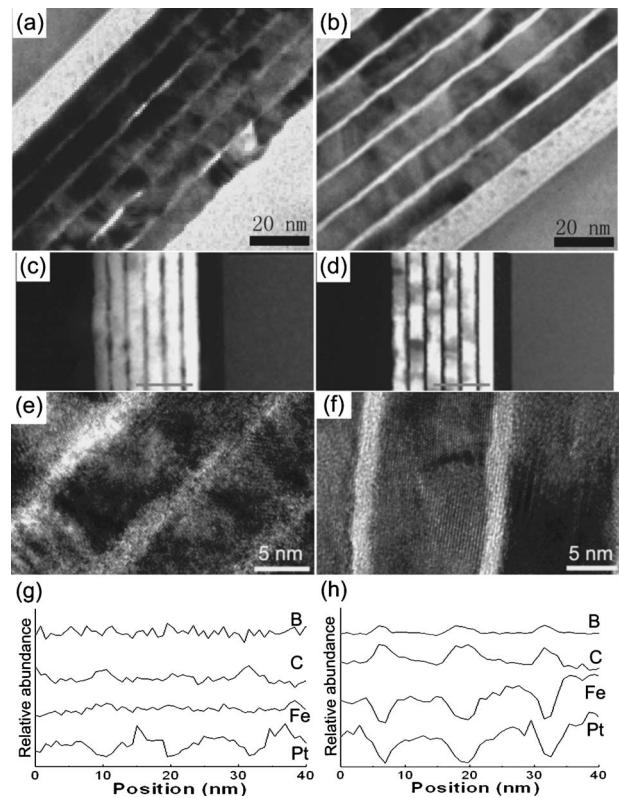


FIG. 2. [(a) and (b)] Low magnification cross section TEM images; [(c) and (d)] high angle annular dark field images; [(e) and (f)] high-resolution images; [(g) and (h)] line scan profiles for multilayer film samples with B_4C layer thicknesses = 1, and 4 nm, respectively.

to firstly take place during the deposition process. The rough interfaces between the individual layers as observed are direct evidence of the island growth mode. The intermixing is further promoted during the postannealing process, when the temperature is raised to 500°C , and diffusion of various compositional elements occurs.

The experimental evidences suggest more significant diffusion of Fe, compared to that of Pt. This is reasonable when one considers the smaller atomic radius of Fe (0.126 nm) than that of the Pt (0.139 nm), which provides a higher mobility of Fe particularly when the B_4C layer is not continuous at low layer thickness. On the other hand, diffusions of B and C are easy due to their small atomic radius and the polycrystalline nature of the FePt layer. Indeed, EELS line scan results suggest the presence of B and C even in the interior of the FePt layer, where they should be absent. Nevertheless, in the EELS measurement, the B and C signals from the FePt layer are not clearly detected when the B_4C layer thickness is smaller than 2 nm, likely due to the finite amount of B and C available in the composite film.

It is interesting to note the FePt grain size dependence on the B_4C layer thickness. Larger grain size is observed when the amount of B and C in the FePt layer is small (signal nondetectable at 1 nm B_4C layer thickness and weak signal detectable at 2 nm B_4C layer thickness). Drop in the grain size occurs at B_4C layer thickness increasing to 3 nm and above, when the signals of B and C become obvious in the FePt layer. Nevertheless, further increase in the B_4C layer thickness (>3 nm) seems to have little effect on promoting B and C diffusions into the FePt layer, and thus further decrease the FePt grain size.

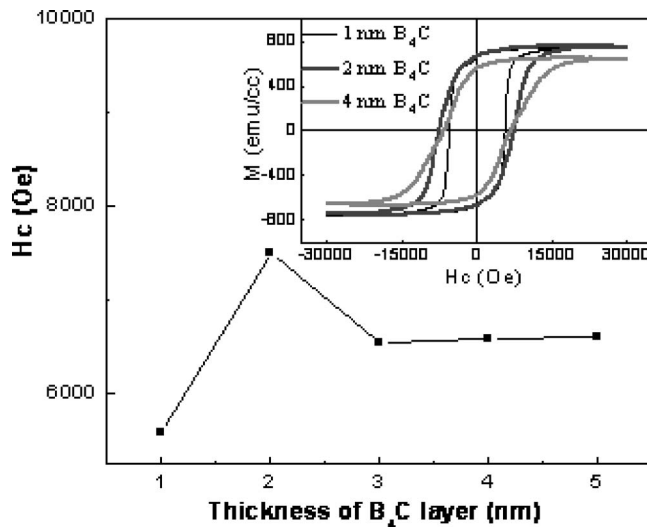


FIG. 3. Plot of the film H_c as a function of B_4C layer thickness. The hysteresis loops of several multilayer films with 1, 2, and 4 nm B_4C layer are shown in the inset of the figure.

The magnetic properties of the composite films have a strong dependence on the B_4C layer thickness. Several hysteresis loops of different B_4C layer thicknesses can be found in the inset of Fig. 3. The coercivities of the composite films as a function of the B_4C layer thicknesses in each period are also plotted in Fig. 3. As the thickness of the B_4C layer increases, the film coercivity first increases before it decreases drastically and eventually levels off at further B_4C layer thickness increase.

The exchange interactions among the magnetic grains (counting both interlayer and intergrain interactions) of the composite films are measured by the δM plot (Fig. 4), which is defined as $\delta M(H) = M_d(H)/M_s - [1 - 2M_r(H)/M_s]$, where, $M_d(H)$ is the dc-demagnetization remanence curve and $M_r(H)$ is the isothermal remanence curve.¹⁷ A strong positive peak is observed in the composite film with 1 nm B_4C layer thickness, indicating strong exchange coupling existing among the FePt particles in such composite film.¹⁸ As the B_4C layer grows thicker, the positive peak in the δM plot becomes much weaker, suggesting the effectively reduced exchange coupling in these composite films.

As the B_4C layer thickness increases from 1 to 2 nm, the improved coercivity of the composite film can be ascribed to (i) the better confinement of Fe atoms in the FePt layer, resulting in a closer 1/1 ratio of Fe/Pt and thus more completed phase transformation to the fct phase, associating

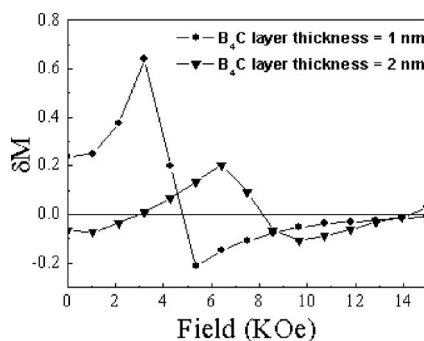


FIG. 4. δM curves for $B_4C/FePt$ composite films with 1 and 2 nm B_4C layer thicknesses.

with higher coercivity; (ii) the complete separation of the FePt layer as well as the B and C atoms in the FePt layer contributes to the isolation of the FePt grains, leading to the weakened exchange coupling in the composite film. Further increase in the B_4C layer thickness above 2 nm results in more B and C diffusions into the FePt layer (evident by the stronger B and C signals identified in the FePt layers, particularly in the samples with larger B_4C layer thickness), leading to suppression of the FePt grain growth. Consequently, the smaller grains result in the decrease in the films' coercivities.¹⁹

In conclusion, we find that B and C in the multilayer composite film have several effects on their structure and magnetic properties. The continuous B_4C layer results in complete separation of the successive FePt layers, which configuration can give satisfactory small grain size (8.8 nm), midhigh coercivity (7500 Oe), low exchange coupling, and reasonable nanoindentation hardness for potential application in the high-density recording. On the one hand, the thicker B_4C layer effectively separates the individual magnetic layers, confines the Fe into the FePt layer, and induces the intermixing of B and C into such layers, leading to effective FePt grain separation. All these factors contribute to the improved magnetic properties of the sample. On the other hand, increased intermixing of B and C into the FePt layer suppresses its grain growth and eventually causes a decrease in the film coercivity.

This work is supported by the Research Grants Council of Hong Kong SAR (Ref. No. CUHK4182/04E), the National Nature Science Foundation of China (No. 50371056), and the Natural Science Foundation Creative Team Project of Hubei Province.

- ¹B. M. Lairson, M. R. Visokay, R. Sinclair, and B. M. Clemens, *Appl. Phys. Lett.* **62**, 639 (1993).
- ²A. Cebollada, D. Weller, J. Sticht, G. R. Harp, R. F. C. Farrow, R. F. Marks, R. Savoy, and J. C. Scott, *Phys. Rev. B* **50**, 3419 (1994).
- ³R. F. C. Farrow, D. Weller, R. F. Marks, M. F. Toney, S. Hom, G. R. Harp, and A. Cebollada, *Appl. Phys. Lett.* **69**, 1166 (1996).
- ⁴J. U. Thiele, L. Folks, M. F. Toney, and D. Weller, *J. Appl. Phys.* **84**, 5686 (1998).
- ⁵R. F. C. Farrow, D. Weller, R. F. Marks, M. F. Toney, D. J. Smith, and M. R. McCartney, *J. Appl. Phys.* **84**, 934 (1998).
- ⁶M. H. Hong, K. Hono, and M. Watanabe, *J. Appl. Phys.* **84**, 4403 (1998).
- ⁷M. Watanabe, T. Nakayama, K. Watanabe, T. Hirayama, and A. Tonomura, *Mater. Trans., JIM* **37**, 489 (1996).
- ⁸N. Li and B. M. Lairson, *IEEE Trans. Magn.* **35**, 1077 (1999).
- ⁹C. H. Park, J. G. Na, P. W. Jang, and S. R. Lee, *IEEE Trans. Magn.* **35**, 3034 (1999).
- ¹⁰B. Bian, K. Sato, Y. Hirotsu, and A. Makino, *Appl. Phys. Lett.* **75**, 3686 (1999).
- ¹¹B. Bian, D. E. Laughlin, K. Sato, and Y. Hirotsu, *J. Appl. Phys.* **87**, 6962 (2000).
- ¹²T. Maeda, T. Kai, A. Kikitsu, T. Nagase, and J. Akiyama, *Appl. Phys. Lett.* **80**, 2147 (2002).
- ¹³Y. N. Hsu, S. Jeong, D. E. Laughlin, and D. N. Lambeth, *J. Appl. Phys.* **89**, 7068 (2001).
- ¹⁴K. Sato, B. Bian, T. Hanada, and Y. Hirotsu, *Scr. Mater.* **44**, 1389 (2001).
- ¹⁵S. Takeshi, K. Osamu, and S. Yutaka, *J. Magn. Mater.* **239**, 310 (2002).
- ¹⁶S. Sun, E. E. Fullerton, D. Weller, and C. B. Murray, *IEEE Trans. Magn.* **37**, 1239 (2001).
- ¹⁷P. E. Kelly, K. O'Grady, P. I. Mayo, and R. W. Chantrell, *IEEE Trans. Magn.* **25**, 3881 (1989).
- ¹⁸H. Zeng, S. H. Sun, T. S. Vedantam, J. P. Liu, Z. R. Dai, and Z. L. Wang, *Appl. Phys. Lett.* **80**, 2583 (2002).
- ¹⁹B. D. Cullity, *Introduction to Magnetic Materials* (Addison-Wesley, Boston, 1972), pp. 385–389, pp. 385–P389.